Chromosome-level reference genome assembly for the protected resource plant, *Zenia insignis*

Authors

Si-Yun Chen[1,2,4], Zhi-Yun Yang[1,4], Rong Zang[1,2,3], Hui Liu[1,2,3], Ting-Shuang Yi[1,2]

Affiliations

1. Germplasm Bank of Wild Species, Yunnan Key Laboratory of Crop Wild Relatives Omics, Kunming Institute of Botany, Chinese Academy of Sciences, Kunming 650201, Yunnan, China
2. University of Chinese Academy of Sciences, Beijing 100049, China
3. Key Laboratory of Plant Diversity and Specialty Crops, Chinese Academy of Sciences, Beijing 100093, China
4. these authors contributed equally: Si-Yun Chen and Zhi-Yun Yang.

corresponding author(s): Hui Liu (Liuhui1@mail.kib.ac.cn), Ting-Shuang Yi (tingshuangyi@mail.kib.ac.cn)

Abstract

Zenia insignis Chun, from the subfamily Dialioideae of Fabaceae, is a tree species of significant economic and ecological values. It is a threatened species as per the IUCN Red List. The absence of a reference genome has impeded research on *Z. insignis* despite its importance. In this study, we generated a reference genome for *Z. insignis*, with a contig N50 of 6.02Mb, a total length of 361.11 Mb, and 97.71% of the sequences assembled into 14 pseudo-chromosomes. The BUSCO assessment score for completeness is 97.30%, and the LAI index assessment score for continuity is 14.57. To our knowledge, this is the first reported genome of a species within the subfamily Dialioideae. The reference genome will provide a valuable resource for the phylogenomic studies of the Fabaceae family and facilitate further research on *Z. insignis*.

Background & Summary

Zenia insignis Chun, a member of the family Fabaceae, is a tree species recognized as one of the Grade-II Wild Plants of National Priority Protection in China[1] and is listed as Near Threatened (NT) on the International Union for Conservation of Nature (IUCN) Red List[2]. This species was named by the renowned botanist Woon-Young Chun in honor of Hongjun Ren (H.C. Zen)[3]. The species is primarily distributed in southern and southwestern China at an altitude range of 200–1000 meters and northern Vietnam[4]. *Zenia insignis* boasts a robust root system and strongly resists drought and infertile conditions[5]. In the karst regions of southern and southwestern China, it has been utilized as an outstanding tree species for afforestation on rocky terrain and as a pioneering species for the control of rocky desertification[5-7]. Additionally, it has significant economic value. The wood of *Z. insignis* is versatile and suitable for producing a range of items, including doors, boards, agricultural implements, and

furniture[8,9]. The plant's tender leaves serve a dual purpose, being used as livestock feed and green manure in rice fields[7-9].

Research on *Z. insignis* has predominantly concentrated on seedling[10,11], reforestation technologies[5,6], and phylogenetic studies[12-19]. Though partial and complete plastome sequences[12-14,16] and nuclear sequences[15,17-19] have been utilized in constructing the phylogenetic tree of the Fabaceae family, the deep phylogenetic relationships within Fabaceae remain to be fully elucidated. A chromosome-level genome sequence of *Z. insignis* would be instrumental in clarifying these phylogenetic relationships. In this study, we have successfully obtained the reference genome of *Z. insignis* and performed comparative analyses with other representative plant genomes to further our understanding of the evolutionary history of the Fabaceae family.

In our study, we integrated multiple sequencing data types to assemble and annotate the genome of *Z. insignis*. Specifically, we used PacBio continuous long reads (CLR) (174.14 Gb, 363.43× coverage), next-generation sequencing (NGS) reads (44.14 Gb, 91.96× coverage), Hi-C data (59.63 Gb, 124.45× coverage), and full-length transcriptome reads (81.92Mb). The resulting reference genome consists of 14 pseudo-chromosomes and spans a total length of 352.84 Mb with a contig N50 of 6.02 Mb. The genome's LAI index score is 14.57. The GC content of the genome is 34.38%, and the proportion of repeat sequences is 35.47%, with long terminal repeat (LTR) elements being the most prevalent, accounting for 9.03%. We also obtained the chloroplast genome sequence of *Z. insignis* with a length of 159,390 bp.

We predicted 33,322 gene models, of which 90.46% (30,143) were functionally annotated. Analysis of orthologous genes between *Z. insignis* and ten other representative plant species revealed 608 orthogroups, with at least 72.72% of species having single-copy genes in any given orthogroup. Additionally, 1,625 gene families underwent significant expansion, and 741 gene families underwent significant contraction in *Z. insignis*. In the whole genome duplication analysis, two collinear block *Ks* peaks were observed at 0.245±0.001 and 1.693±0.001, suggesting that *Z. insignis* has undergone an additional whole genome duplication (WGD) event after the γ WGT event shared by all core eudicots.

Methods

Genome size estimation and sequencing

Fresh young leaves of *Z. insignis* were collected from the Kunming Botanical Garden (KBG), Kunming Institute of Botany, Chinese Academy of Sciences (KIB), Yunnan Province, China. The leaves were immediately flash-frozen in liquid nitrogen to preserve their cellular structure and molecular content. Subsequently, the samples were transferred to an ultra-low temperature freezer maintained at –80°C for storage.

DNA/RNA extraction, library construction, and sequencing processes were provided by Wuhan Frasergen Bioinformatics Co., Ltd. The major steps are summarized below:

77 1. Genomic DNA was extracted from the tender leaves of *Z. insignis* using the modified
78 cetyltrimethylammonium bromide (CTAB) method[20,21]. Total RNA was isolated using a Trizol
79 reagent (Invitrogen, CA, USA). The quantity and quality of the DNA/RNA were determined
80 using a NanoDrop 2000 spectrophotometer (NanoDrop Technologies, Wilmington, DE, USA).

81 2. The quality-compliant DNA was further tested for purity and integrity using 0.8% agarose
82 gel electrophoresis and a Qubit dsDNA HS Assay Kit on a Qubit 3.0 Fluorometer (Life
83 Technologies, Carlsbad, CA, USA). RNA contamination was identified using a 1.5% agarose gel,
84 and purity and integrity were evaluated using a NanoDrop 2000 and a Bioanalyzer 2100
85 system (Agilent Technologies, CA, USA).

86 3. According to the manufacturer's instructions, a short-read library was constructed using
87 the VAHTS Universal DNA Library Prep Kit (Vazyme, Nanjing, China) for MGI. The library's
88 quantification and sizing were measured using a Qubit 3.0 Fluorometer and a Bioanalyzer
89 2100 system (Agilent Technologies, CA, USA). Paired-end sequencing of the short-read library
90 was conducted on an MGI-SEQ 2000 platform (BGI, China).

91 4. To perform long-read sequencing, the library was prepared in accordance with the
92 PacBio single-molecule real-time (SMRT) protocol and then sequenced on a Pacific Biosciences
93 Sequel II System in CLR mode.

94 5. The construction of the Hi-C library commenced with the cross-linking of fresh leaves of
95 *Z. insignis* under vacuum infiltration with 3% formaldehyde. Following lysis, digestion,
96 labelling, ligation, purification, adaptor addition, and PCR amplification, the Hi-C libraries were
97 quantified and sequenced on the MGI-SEQ 2000 platform.

98 6. For short-read transcriptome sequencing, RNA was isolated from Z. insignis young leaves
99 using the QIAGEN kit according to the manufacturer's instructions. The short-read library was
100 subsequently constructed and sequenced on the MGI-SEQ 2000 platform using paired-end
101 sequencing.

102 7. The full-length transcriptome sequencing was conducted using the Pacific Biosciences
103 DNA Template Prep Kit 2.0 for library construction (Pacific Biosciences, CA, USA).
104 Subsequently, the SMRT sequencing was performed on a Pacific Biosciences Sequel II platform.

105 Our study generated 44.14 Gb of raw data for the whole genome, 174.14 Gb of PacBio CLR
106 data, 59.63 Gb of Hi-C data, and 81.92 Mb of full-length transcriptome data (Table 1).

107 The genome size of *Z. insignis* was assessed using flow cytometry analysis conducted on a
108 BD FACScalibur flow cytometer (BD Biosciences). The test sample preparation was
109 conducted in accordance with the manufacturer's guidelines and aligned with established
110 methodologies from previous literature[22,23]. As a standard reference, we utilized *Zea mays*
111 (maize)[24], a species with a well-documented genome size of 2.3 Gb. The analysis yielded a

112 result indicating that the genome size of *Z. insignis* is approximately 480 ± 4.8 Mb (Figure
113 1A).

114 A *K-mer* analysis was conducted on *Z. insignis* to estimate its genome size. Next-
115 generation sequencing (NGS) data was obtained from Frasergen and processed Fastp
116 v0.19.3[25]. This involved the removal of adapter sequences, the filtration of reads deemed to
117 be of insufficient length, and the elimination of those with low quality. Subsequently,
118 Jellyfish v2.2.10[26] was employed to calculate the frequency distribution of the cleaned data
119 using 21-*mers*. Subsequently, GenomeScope v2.0[27] was employed to estimate the
120 fundamental characteristics of the genome. The genome size of *Z. insignis* was estimated to
121 be approximately 364.94 Mb, with a heterozygosity rate of 0.842% and a repeat content of
122 1.17% (Figure 1B).

123 ***De novo* genome assembly**

124 Figure 2 illustrates the methodology employed for the chromosome-level genome assembly
125 of *Z. insignis*. The objective was to utilize three distinct assemblers, compare their resulting
126 assemblies, and achieve a high-quality assembly. The assemblers employed were Falcon
127 v0.3.0[28], Canu v2.1.1[29], and Flye v2.9[30]. The following section provides a summary of the
128 assembly process.

129 1. The Falcon software was employed to assemble the CLR long reads. The resulting
130 contigs were then polished using long reads with GCpp v2.0.0[31]. Subsequently, the processes
131 above yielded the assembly contig, designated as Assembly_Contig1. Subsequently,
132 Assembly_Contig1 was subjected to further refinement with short reads, employed
133 NextPolish v1.31[32]. The output from the process was designated as the "Falcon contig". To
134 eliminate redundancy, the Falcon contig was processed with Purge_Dups v1.2.5[33], and the
135 resulting non-redundant contigs were designated as the "Falcon_purge contigs".

136 2. The Canu software was employed to assemble the CLR long reads, and the result was
137 subsequently polished with long reads by GCpp. Through these processes, we obtained
138 Assembly_Contig2. Assembly_Contig2 was then polished with short reads using NextPolish,
139 with the output from this step designated as the "Canu_contig". The Canu_contig was
140 subsequently subjected to further processing to eliminate redundancy, with the result that
141 the non-redundant contigs were designated as the “Canu_purged contigs". Purge_Dups also
142 employed the process of eliminating redundancy.

143 3. The third assembler employed was Flye, which accepted the error-corrected reads
144 generated by Canu as input. The output from Flye was polished with long reads by GCpp,
145 resulting in the generation of Assembly_Contig3. Subsequently, the contig was polished with
146 short reads using NextPolish, resulting in the "Flye_contig". The Flye_contig was subjected to
147 a process of redundancy elimination using Purge_Dups, resulting in the generation of a set
148 of non-redundant contigs designated as the "Flye_purge contigs".

149 4. Six distinct results were obtained after completing the three steps above. The
150 following contigs were identified: Falcon contig, Canu contig, Flye_contig, Falcon_purge
151 contig, Canu_purge contig, and Flye_purge contig.

152 BUSCO v5.4.5[34] with 1614 embryophyta single-copy orthologs was employed to assess
153 the completeness of the assembly, the N50[35] metric provided insights into the distributions
154 of contigs, and the LTR Assembly Index (LAI) v2.9.0[36] was employed to evaluate the
155 contiguity of the assembled genome. The results are presented in Tables 2–4. Notably, the
156 Canu_purged assembly exhibited the highest N50 value, the Flye_purged assembly achieved
157 the optimal BUSCO score, and the Falcon_purged contig assembly exhibited the highest LAI
158 score. In other words, the result generated by Purge_Dups exhibited a better contiguity.
159 Manual inspection using Hi-C reads revealed a low redundancy in Falcon_purge assembly
160 (Supplementary Figure 1). Consequently, the results generated by Purge_Dups were
161 selected for further comparison. A comparison of the Falcon_purge assembly with other
162 results generated by Purge_Dups revealed that it exhibited high contiguity with N50 of 6.02
163 Mb, BUSCO completeness of 97.30%, and LAI score of 14.57.

164 During the chromosome assembly phase, we integrated Hi-C data with the previously
165 assembled contigs to achieve chromosome-level scaffolding. Specifically, Juicer was
166 employed to align the Hi-C reads to the contig genome. Subsequently, the 3D-DNA pipeline[37]
167 was used to map the contigs onto chromosome-level scaffolds. For a visual representation of
168 the Hi-C data, Juicebox v1.22[37] was employed. The results of the chromosome assembly also
169 demonstrated that the Purge_Dups results exhibited lower redundancy, compared to the
170 rest two assemblies (Supplementary Figure 1). The Purge_Dups result was chosen as the
171 optimal choice, and subsequently, the heatmap of the result was manually adjusted (Figure
172 3A). The final outcome of this process was the generation of 14 pseudo-chromosomes with a
173 total length of 352.84 Mb, as illustrated in Figures 3A and 3B.

174 The GetOrganelle v1.7.3.3[38] software was employed to assemble the chloroplast genome,
175 successfully acquiring the complete chloroplast genome sequence depicted in Figure 3C. The
176 newly assembled chloroplast genome spans 159,390 base pairs (bp) and is annotated using
177 the PGA tool[39], as shown in Figure 3C, drawn by OGDRAW v1.3.1[40]. For comparative analysis
178 of the chloroplast genome, we employed the MAFFT plugin within the Geneious Prime
179 software suite[41] to align our sequence with a published chloroplast genome of *Z. insignis*[16]
180 (NC_045299.1) obtained from the National Center for Biotechnology Information(NCBI). As
181 illustrated in Figure 3D, the alignment result revealed that apart from some single nucleotide
182 polymorphisms (SNPs) in non-coding regions, there were no significant differences in large-
183 scale sequences.

184 **Repeat annotation**

185 The RepeatModeler v2.0.1[42] software was employed to predict the occurrence of repeat
186 sequences within the genome of *Z. insignis*. RepeatModeler integrates three *de novo* repeat-
187 finding programs: RECON v1.08[43], RepeatScout v1.0.6[44], and LTRHarvest v5.9[45]/LTR_retriever

188 v2.9.0[46]. For our analysis, we employed rmblast v2.13.0[47] as the search engine.
189 Subsequently, the output from RepeatModeler was processed using RepeatMasker v4.1.4[48]
190 to identify and mask the repetitive elements within the *Z. insignis* genome.

191 Table 5 presents the results of the repeat sequence analysis for *Z. insignis*. A total of
192 128.08 Mb was identified as repetitive sequences, constituting 35.47% of the pseudo-
193 chromosome sequences. The analysis revealed four primary classes of transposable
194 elements within the genome: 9.03% for long terminal repeats (LTRs), 3.08% for DNA
195 elements, 1.81% for long interspersed nuclear elements (LINEs), and 0.08% for short
196 interspersed nuclear elements (SINEs).

197 **Gene prediction and functional annotation**

198 A hybrid approach was implemented to achieve high-quality gene prediction, incorporating
199 *de novo* prediction, homology-based prediction, and RNA-Seq-assisted prediction. The
200 AnnoSmk v1.0[49] pipeline was employed for gene prediction. Firstly, the RepeatMasker
201 v4.1.4[48] software was employed to generate repeat evidence. For homology-based
202 prediction, protein data for *Arabidopsis thaliana*[50] was sourced from The Arabidopsis
203 Information Resource (TAIR) and employed to construct homologous gene models using
204 genBlastG v1.38[51] as protein evidence. For transcriptome evidence, HISAT2 v2.2.1[52] was
205 employed to map paired-end short transcriptome reads to the *Z. insignis* genome. Then, the
206 mapped reads were assembled using Trinity v2.11.0[53]. Concurrently, we processed full-
207 length transcriptome data with the IsoSeq3 v3.4.0[54] pipeline to produce high-quality
208 consensus transcript sequences. Minimap2 v2.22[55] was employed to align both short and
209 long-read data, from which the transcriptome evidence was derived. The integrated repeat,
210 protein, and transcript evidence were then subjected to gene prediction using MAKER2
211 v3.01.03[56]. Three rounds of MAKER2 analysis were executed. In the second and third rounds,
212 the output generated through *de novo* gene prediction using AUGUSTUS v3.4.0[57] was also
213 included. BUSCO was employed to evaluate the gene prediction results after each round of
214 MAKER2, yielding scores of 46.60%, 96.60%, and 96.80%, respectively (Table 6). Following
215 the third round of MAKER2, the results were input into the PASA pipeline v2.5.0[58], resulting
216 in the final output. The final BUSCO score for the AnnoSmk pipeline was 97.20% (Table 6). In
217 conclusion, a total of 33,322 gene models were predicted.

218 The functional annotation of protein-coding genes was conducted using the eggNOG-
219 mapper website[59], which employs the eggNOG-mapper v2.1.12[60] and the eggNOG 5
220 database. This tool utilizes several comprehensive databases, including Pfam[61], InterPro[62],
221 Gene Ontology (GO)[63], and the Kyoto Encyclopedia of Genes and Genomes (KEGG)[64], to
222 annotate protein sequences. This analysis resulted in the successful functional annotation of
223 30,143 protein-coding genes, representing 90.46% of the total gene models.

224 **Comparative genomics and phylogenetic analysis**

225 The identification of orthologous genes represents a central objective in the fields of
226 comparative genomics and phylogenetics. In this study, we compared the protein sequences
227 of *Z. insignis* with those of ten other representative plant species, including *Arabidopsis*
228 *thaliana*[50](GCA_000001735.2), *Cercis chinensis*[65](PRJCA007288), *Eriobotrya*
229 *japonica*[66](GWHAAZU00000000.1), *Glycine max*[67](GCA_000004515.5), *Lysidice*
230 *rhodostegia*[68], *Medicago truncatula*[69](GCA_003473485.2), *Senna tora*[70](GCA_014851425.1),
231 *Quercus mongolica*[71](GCA_011696235.1), *Vitis vinifera*[72](GCA_030704535.1), and *Polygala*
232 *tenuifolia*[73](TCMPG20196). These were employed to discern orthologs and paralogs. The
233 OrthoFinder v2.5.4[74] software was used to predict orthologous and paralogous gene
234 families. The protein sequences from the eleven species were input into OrthoFinder,
235 resulting in the clustering of 39,196 genes into 30,977 gene families. The analysis revealed
236 8,698 orthogroups that are shared by all species. Of these, 40 orthogroups comprise single-
237 copy genes, while 608 orthogroups have at least 72.72% of species exhibiting single-copy
238 genes within each orthogroup.

239 We used the 608 orthogroups obtained from our analysis to construct phylogenetic trees.
240 Initially, the seqkit tool v0.16.1[75] was employed to extract the corresponding nucleic acid
241 sequences. Subsequently, the DNA sequences were aligned using MUSCLE v3.81511[76], and
242 the sequences were concatenated using seqkit to generate a supermatrix of genes. The
243 supermatrix was subsequently employed as the input for constructing the phylogenetic tree,
244 which was generated using RAxML v8.2.12[77] with the maximum likelihood method. The most
245 appropriate model for RAxML, GTR+F+R3, was determined using IQTree v2.1.4-beta[78].
246 Subsequently, the divergence times at the nodes of the phylogenetic tree using R8s v1.81,
247 with calibration time points derived from the TimeTree database[79]. The calibration points
248 included the divergence times between *M. truncatula* and *G. max* (55 million years ago,
249 MYA), *M. truncatula* and *L. rhodostegia* (68 MYA), and *G. max* and *L. rhodostegia* (68 MYA).
250 Finally, the CAFE v5.0[80] program was employed to understand the expansion and contraction
251 of gene families across the phylogenetic tree. The results indicate that *Z. insignis* (subfamily:
252 Dialioideae) diverged from *S. tora* (subfamily: Caesalpinioideae) and *M. truncatula*
253 (subfamily: Papilionoideae) around 51 MYA. The analysis of gene family dynamics identified
254 1,625 gene families with significant expansion(p<0.05) and 741 gene families with significant
255 contraction(p=0.05) in the genome of *Z. insignis* (Figure 4A).

256 We conducted GO and KEGG enrichment analyses to understand the biological
257 significance of the gene families that exhibited significant expansion and contraction with *a*
258 *P- value* cutoff of 0.05. The GO and KEGG analyses were performed using the eggNOG-
259 mapper web platform[59]. We employed TBtools v2.086[81] to carry out the enrichment analysis
260 of the identified gene families. The GO enrichment analysis revealed that the families that
261 exhibited significant expansion were predominantly involved in molecular function and
262 biological process (Supplementary Figure 2A). The terms of the molecular function are
263 mainly 'metal ion transmembrane transporter activity', 'inorganic cation transmembrane
264 transporter activity', and 'cellulose synthase activity' (Supplementary Figure 2A). And the
265 terms of the biological process are mainly 'hydrocarbon metabolic process' and 'olefin
266 metabolic process' (Supplementary Figure 2A). Furthermore, the KEGG enrichment analysis

267 revealed that these families are significantly enriched in pathways such as 'alpha-Linolenic
268 acid metabolism', 'MAPK signaling pathway-plant', 'metabolism of terpenoids and
269 polyketides', 'biosynthesis of other secondary metabolites', and 'ion channels'
270 (Supplementary Figure 2C). Conversely, for the families that exhibited a significant
271 contraction, the GO enrichment analysis was predominantly involved in the biological
272 process of 'embryo development ending in seed dormancy', 'embryo development', 'seed
273 development', 'fruit development', and 'proteolysis involved in protein catabolic process'
274 (Supplementary Figure 2B). The corresponding KEGG enrichment analysis identified
275 pathways including 'protein families: metabolism', 'ubiquitin mediated proteolysis',
276 'chromosome and associated proteins', 'protein processing in endoplasmic reticulum', and
277 'brite hierarchies' (Supplementary Figure 2D).

278 **Identification of whole genome duplication events**

279 To elucidate the whole genome duplication (WGD) events in *Z. insignis*, a comprehensive
280 analysis was conducted using the WGDI toolkit v0.6.5[82] with various parameters. We used *V.*
281 *vinifera*[72] as a reference genome. First, we used BLAST+ v2.15.0[83] to identify homologous
282 genes (e-value 10^{-5}). We then drew a dot plot of collinear genes with the parameter -d (Figure
283 5A and B). Next, we conducted a collinear analysis with the parameter -icl, calculated *Ks* values
284 with the parameter -ks, combined the results of the collinear analysis and *Ks* values with the
285 parameter -bi, and fitted *Ks* peaks with the parameter -pf. Finally, we plotted a *Ks* dot plot
286 with the parameter -bk (Figure 5C and D) and a *Ks* peak plot with the parameter -kf (Figure
287 4B). The dot-plot and *Ks* dot-plot results for *Z. insignis* showed a high degree of similarity to
288 those shown in Figure 4A and C. They were cross-validated with the results from *V. vinifera* in
289 Figure 5B and D. The *Ks* peak analysis revealed two peaks at 0.245±0.001 and 1.693±0.001,
290 suggesting that *Z. insignis* likely experienced a lineage-specific WGD event, as illustrated in
291 Figure 4B.

292 Technical Validation

293 As part of our sequencing pipeline, we conducted a rigorous sample quality assessment for
294 both DNA and RNA samples used in the study. The specific procedures and criteria for this
295 assessment are detailed in our paper's 'Methods' section, ensuring that only high-quality
296 samples were selected for subsequent sequencing and analysis.

297 In our study, we employed two distinct methodologies to estimate the genome size of *Z.*
298 *insignis*. The first method involved Flow cytometry analysis, which provided a quick and
299 accurate measurement of the relative DNA content within the cells of *Z. insignis*. The second
300 method was *K-mer* analysis, which leverages the frequency distribution of DNA sequences to
301 predict genome size. The details have been mentioned in the Method section. Both
302 approaches were crucial in validating the genome size and ensuring the reliability of our
303 genomic data.

In our assessment of the *de novo* genome assembly for *Z. insignis*, we utilized a suite of metrics, including N50, BUSCO, and LAI, to evaluate the performance of various assembly software tools. The results of these evaluations are presented in Tables 2, 3, and 4, which compare the assembly quality, completeness, and continuity across different assemblers. Based on these assessments, Falcon-purged output demonstrated the most favorable balance of completeness and continuity, making it the choice for subsequent downstream analyses. In summary, we have successfully generated a high-quality reference genome for *Z. insignis*, which may promote further biological and comparative genomic studies of this species.

Code Availability

We used all software or pipelines, depending on the tools' manuals or protocols. The software's version is described in the methods section, and the parameters are given if not default.

Acknowledgements

This research was supported by the Major Program for Basic Research Project of Yunnan Province (202401BC070001), the Youth Talents Special Project of Yunnan Province "Xingdian Talents Support Program"(XDYC-QNRC-2022-0423), the National Natural Science Foundation of China, key international (regional) cooperative research project (No. 31720103903), Yunnan Provincial Basic Research Program Youth Project (2019FD058), and National Natural Science Foundation of China (No. 32270247). We are grateful to the Germplasm Bank of Wild Species, particularly the Molecular Biology Experiment Center and the iFlora High Performance Computing Center, the Kunming Botanical Garden, Ms. Ding-Jie Wang, and Mr. Zuo-Ying Xiahou.

Author contributions

T.-S. Y. and H. L. Designed the experiments. S.-Y. C. and Z.-Y. Y. performed the experiments. S.-Y. C., H. L., and R. Z. analyzed the data. S.-Y. C., T.-S. Y. and H. L. wrote the paper. All Authors read and approved the manuscript.

Competing interests

The authors declare no competing interests.

References

1. the State Council. *List of Wild Plants of National Priority Protection(First batch)*, <https://www.gov.cn/gongbao/content/2000/content_60072.htm> (2000).
2. IUCN. *The IUCN Red List of Threatened Species*, <http://www.iucnredlist.org/> (2024).
3. Chun, W.-Y. A new genus in the Chinese flora. *Sunyatsenia* **6**, 196–198 (1946).
4. Xu, L.-R. *et al. Fabaceae(Leguminosae)* In *Flora of China* Vol. 10. Wu, Z.-Y., Raven, P. H., & Hong, D.-Y. Eds 27(Science Press & Missouri Botanical Garden Press, 2010).

5. Ao, H., He, D., Zhang, Z., Xia, H. & Yang, W. *Zenia insignis* communities in limestone areas of Guangdong. *Tropical Geography* **17**, 275–276+278–282, http://dx.chinadoi.cn/10.13284/j.cnki.rddl.000227 (1997).
6. Zhang, Z.-P., He, D.-Q., Ao, H.-X., Yang, W.-J. & Wu, H.-M. The characteristic of physiological ecology of the main tree species used for afforestation at limestone regions in North Guangdong. *Acta Phytoecol. Sin.* **17**, 133–142 (1993).
7. Zhang, Y. Growth performance on acid soil and cultivation technique of *Zenia insignis*. *Guangdong Forestry Science and Technology* **23**, 76–79, http://dx.chinadoi.cn/10.3969/j.issn.1006-4427.2007.01.016 (2007).
8. Hou, L., Li, Y., Li, P., Yang, Y. & Xie, Y. Study of *Zenia insignis* Chun. comprehensive utilization. *Sci. Silvae Sin.* **37**, 139–143, http://dx.chinadoi.cn/10.11707/j.1001-7488.20010322 (2001).
9. Yu, G. & Zhang, Y. A preliminary study on the wood fibre form of *Zenia insignis* introduced in Fujian Province. *Journal of Fujian Forestry Science and Technology* **25**, 31–33, http://dx.chinadoi.cn/10.3969/j.issn.1002-7351.1998.01.006 (1998).
10. Qin, Y.-R., Jiang, G.-M., Cen, Z.-Y., Chen, Y.-S. & Lan, C.-Y. Research on the seed's germination characteristic of *Zenia insignis* as the vanguard tree for afforestation in karst areas. *Seed* **27**, 15–21, http://dx.chinadoi.cn/10.3969/j.issn.1001-4705.2008.12.005 (2008).
11. Tang, W., Pan, B., Wei, H., Huang, Z. & Lu, Q. Comparative study on the characteristics of seed germination and seedling growth of different *Zenia insignis* provenances in Guangxi. *Seed* **38**, 93–98, http://dx.chinadoi.cn/10.16590/j.cnki.1001-4705.2019.12.93 (2019).
12. Bai, H.-R., Oyebanji, O., Zhang, R. & Yi, T.-S. Plastid phylogenomic insights into the evolution of subfamily Dialioideae (Leguminosae). *Plant Diversity* **43**, 27–34, https://doi.org/10.1016/j.pld.2020.06.008 (2021).
13. Herendeen, P. S. *Phylogenetic Relationships in Caesalpinioid Legumes: A Preliminary Analysis Based on Morphological and Molecular Data* In *Advances in legume systematics, part 10* Klitgaard, B. B. & Bruneau, A. Eds 37–62 (Royal Botanic Gardens, 2003).
14. Kajita, T., Ohashi, H., Tateishi, Y., Bailey, C. D. & Doyle, J. J. rbcL and legume phylogeny, with particular reference to Phaseoleae, Millettieae, and Allies. *Syst. Bot.* **26**, 515–536, http://dx.doi.org/10.1043/0363-6445-26.3.515 (2001).
15. Koenen, E. J. M. *et al.* Large-scale genomic sequence data resolve the deepest divergences in the legume phylogeny and support a near-simultaneous evolutionary origin of all six subfamilies. *New Phytol.* **225**, 1355–1369, https://doi.org/10.1016/j.molp.2021.02.006 (2020).
16. Lai, Q., Tu, T. & Zhang, D. The complete plastid genome of *Zenia insignis* Chun (Leguminosae). *Mitochondrial DNA Part B-Resour.* **4**, 2926–2927, https://doi.org/10.1080/23802359.2019.1660266 (2019).
17. The Legume Phylogeny Working Group. A new subfamily classification of the Leguminosae based on a taxonomically comprehensive phylogeny. *Taxon* **66**, 44–77, https://doi.org/10.12705/661.3 (2017).
18. Zhang, R. *et al.* Exploration of plastid phylogenomic conflict yields new insights into the deep relationships of Leguminosae. *Syst. Biol.* **69**, 613–622, https://doi.org/10.1093/sysbio/syaa013 (2020).

383 19. Zhao, Y. *et al.* Nuclear phylotranscriptomics and phylogenomics support numerous
384 polyploidization events and hypotheses for the evolution of rhizobial nitrogen-fixing
385 symbiosis in Fabaceae. *Mol. Plant.* **14**, 748–773,
386 https://doi.org/10.1016/j.molp.2021.02.006 (2021).
387 20. Doyle, J. J. & Doyle, J. L. A rapid DNA isolation procedure for small quantities of fresh leaf
388 tissue. *Phytochemical Bulletin* **19**, 11–15 (1987).
389 21. Allen, G. C., Flores-Vergara, M. A., Krasynanski, S., Kumar, S. & Thompson, W. F. A modified
390 protocol for rapid DNA isolation from plant tissues using cetyltrimethylammonium
391 bromide. *Nat. Protoc.* **1**, 2320–2325, https://doi.org/10.1038/nprot.2006.384 (2006).
392 22. Doležel, J., & Bartoš, J. Plant DNA flow cytometry and estimation of nuclear genome size.
393 *Ann. Bot.* **95**, 99–110, https://doi.org/10.1093/aob/mci005 (2005).
394 23. Doležel, J., Greilhuber, J. & Suda, J. Estimation of nuclear DNA content in plants using flow
395 cytometry. *Nat. Protoc.* **2**, 2233–2244, https://doi.org/10.1038/nprot.2007.310 (2007).
396 24. Schnable, P. S. *et al.* The B73 maize genome: complexity, diversity, and dynamics. *Science*
397 **326**, 1112–1115, https://doi.org/10.1126/science.1178534 (2009).
398 25. Chen, S., Zhou, Y., Chen, Y. & Gu, J. fastp: an ultra-fast all-in-one FASTQ preprocessor.
399 *Bioinformatics* **34**, i884–i890, https://doi.org/10.1093/bioinformatics/bty560 (2018).
400 26. Marçais, G. & Kingsford, C. A fast, lock-free approach for efficient parallel counting of
401 occurrences of *k-mers*. *Bioinformatics* **27**, 764–770,
402 https://doi.org/10.1093/bioinformatics/btr011 (2011).
403 27. Ranallo-Benavidez, T. R., Jaron, K. S. & Schatz, M. C. GenomeScope 2.0 and Smudgeplot
404 for reference-free profiling of polyploid genomes. *Nat. Commun.* **11**, 1432,
405 https://doi.org/10.1038/s41467-020-14998-3 (2020).
406 28. Chin, C.-S. *et al.* Phased diploid genome assembly with single-molecule real-time
407 sequencing. *Nat. Methods* **13**, 1050–1054, https://doi.org/10.1038/nmeth.4035 (2016).
408 29. Koren, S. *et al.* Canu: scalable and accurate long-read assembly via adaptive k-mer
409 weighting and repeat separation. *Genome Res.* **27**, 722–736,
410 https://doi.org/10.1101/gr.215087.116 (2017).
411 30. Kolmogorov, M., Yuan, J., Lin, Y. & Pevzner, P. A. Assembly of long, error-prone reads using
412 repeat graphs. *Nat. Biotechnol.* **37**, 540–546, https://doi.org/10.1038/s41587-019-0072-8
413 (2019).
414 31. Seifert, D. & Töpfer, A. *GitHub*, <https://github.com/PacificBiosciences/gcpp> (2021).
415 32. Hu, J., Fan, J., Sun, Z. & Liu, S. NextPolish: a fast and efficient genome polishing tool for
416 long-read assembly. *Bioinformatics* **36**, 2253–2255,
417 https://doi.org/10.1093/bioinformatics/btz891 (2019).
418 33. Guan, D. *et al.* Identifying and removing haplotypic duplication in primary genome
419 assemblies. *Bioinformatics* **36**, 2896–2898,
420 https://doi.org/10.1093/bioinformatics/btaa025 (2020).
421 34. Manni, M., Berkeley, M. R., Seppey, M., Simão, F. A. & Zdobnov, E. M. BUSCO update:
422 novel and streamlined workflows along with broader and deeper phylogenetic coverage
423 for scoring of eukaryotic, prokaryotic, and viral genomes. *Mol. Biol. Evol.* **38**, 4647–4654,
424 https://doi.org/10.1093/molbev/msab199 (2021).
425 35. Lander, E. S. *et al.* Initial sequencing and analysis of the human genome. *Nature* **409**, 860–
426 921, https://doi.org/10.1038/35057062 (2001).

36. Ou, S., Chen, J. & Jiang, N. Assessing genome assembly quality using the LTR Assembly Index (LAI). *Nucleic Acids Res.* **46**, e126–e126, https://doi.org/10.1093/nar/gky730 (2018).
37. Dudchenko, O. *et al. De novo* assembly of the *Aedes aegypti* genome using Hi-C yields chromosome-length scaffolds. *Science* **356**, 92–95, https://doi.org/10.1126/science.aal3327 (2016).
38. Jin, J.-J. *et al.* GetOrganelle: a fast and versatile toolkit for accurate *de novo* assembly of organelle genomes. *Genome Biol.* **21**, 241, https://doi.org/10.1186/s13059-020-02154-5 (2020).
39. Qu, X.-J., Moore, M. J., Li, D.-Z. & Yi, T.-S. PGA: a software package for rapid, accurate, and flexible batch annotation of plastomes. *Plant Methods* **15**, 50, https://doi.org/10.1186/s13007-019-0435-7 (2019).
40. Greiner, S., Lehwark, P. & Bock, R. OrganellarGenomeDRAW (OGDRAW) version 1.3.1: expanded toolkit for the graphical visualization of organellar genomes. *Nucleic Acids Res.* **47**, W59–W64, https://doi.org/10.1093/nar/gkz238 (2019).
41. Kearse, M. *et al.* Geneious Basic: an integrated and extendable desktop software platform for the organization and analysis of sequence data. *Bioinformatics* **28**, 1647–1649, https://doi.org/10.1093/bioinformatics/bts199 (2012).
42. Flynn, J. M. *et al.* RepeatModeler2 for automated genomic discovery of transposable element families. *Proc. Natl. Acad. Sci. U. S. A.* **117**, 9451–9457, https://doi.org/10.1073/pnas.1921046117 (2020).
43. Bao, Z. & Eddy, S. R. Automated *de novo* identification of repeat sequence families in sequenced genomes. *Genome Res.* **12**, 1269–1276, https://doi.org/10.1101/gr.88502 (2002).
44. Price, A. L., Jones, N. C. & Pevzner, P. A. *De novo* identification of repeat families in large genomes. *Bioinformatics* **21**, i351–i358, https://doi.org/10.1093/bioinformatics/bti1018 (2005).
45. Ellinghaus, D., Kurtz, S. & Willhoeft, U. LTRharvest, an efficient and flexible software for *de novo* detection of LTR retrotransposons. *BMC Bioinformatics* **9**, 18, https://doi.org/10.1186/1471-2105-9-18 (2008).
46. Ou, S. & Jiang, N. LTR_retriever: a highly accurate and sensitive program for identification of long terminal repeat retrotransposons *Plant Physiol.* **176**, 1410–1422, https://doi.org/10.1104/pp.17.01310 (2017).
47. Smit, A., Hubley, R. & Rosen, J. *RMBlast*, <https://www.repeatmasker.org/rmblast/> (2024).
48. Chen, N. Using RepeatMasker to identify repetitive elements in genomic sequences. *Curr. Protoc. Bioinf.* **5**, 4.10.11–14.10.14, https://doi.org/10.1002/0471250953.bi0410s05 (2004).
49. Yan, H. & Liu, H. *AnnoSmk*, <https://github.com/yanhui-k/AnnoSmk> (2024).
50. The Arabidopsis Genome, I. Analysis of the genome sequence of the flowering plant *Arabidopsis thaliana*. *Nature* **408**, 796–815, https://doi.org/10.1038/35048692 (2000).
51. She, R. *et al.* genBlastG: using BLAST searches to build homologous gene models. *Bioinformatics* **27**, 2141–2143, https://doi.org/10.1093/bioinformatics/btr342 (2011).

52. Kim, D., Paggi, J. M., Park, C., Bennett, C. & Salzberg, S. L. Graph-based genome alignment and genotyping with HISAT2 and HISAT-genotype. *Nat. Biotechnol.* **37**, 907–915, https://doi.org/10.1038/s41587-019-0201-4 (2019).
53. Grabherr, M. G. *et al.* Full-length transcriptome assembly from RNA-Seq data without a reference genome. *Nat. Biotechnol.* **29**, 644–652, https://doi.org/10.1038/nbt.1883 (2011).
54. Wang, B. *et al.* Unveiling the complexity of the maize transcriptome by single-molecule long-read sequencing. *Nat. Commun.* **7**, 11708, https://doi.org/10.1038/ncomms11708 (2016).
55. Li, H. Minimap2: pairwise alignment for nucleotide sequences. *Bioinformatics* **34**, 3094–3100, https://doi.org/10.1093/bioinformatics/bty191 (2018).
56. Holt, C. & Yandell, M. MAKER2: an annotation pipeline and genome-database management tool for second-generation genome projects. *BMC Bioinformatics* **12**, 491, https://doi.org/10.1186/1471-2105-12-491 (2011).
57. Stanke, M., Diekhans, M., Baertsch, R. & Haussler, D. Using native and syntenically mapped cDNA alignments to improve *de novo* gene finding. *Bioinformatics* **24**, 637–644, https://doi.org/10.1093/bioinformatics/btn013 (2008).
58. Haas, B. J. *et al.* Improving the Arabidopsis genome annotation using maximal transcript alignment assemblies. *Nucleic Acids Res.* **31**, 5654–5666, https://doi.org/10.1093/nar/gkg770 (2003).
59. *eggNOG-mapper*, <http://eggnog-mapper.embl.de/> (2024).
60. Cantalapiedra, C. P., Hernández-Plaza, A., Letunic, I., Bork, P. & Huerta-Cepas, J. eggNOG-mapper v2: functional annotation, orthology assignments, and domain prediction at the metagenomic scale. *Mol. Biol. Evol.* **38**, 5825–5829, https://doi.org/10.1093/molbev/msab293 (2021).
61. Mistry, J. *et al.* Pfam: The protein families database in 2021. *Nucleic Acids Res.* **49**, D412–D419, https://doi.org/10.1093/nar/gkaa913 (2020).
62. Paysan-Lafosse, T. *et al.* InterPro in 2022. *Nucleic Acids Res.* **51**, D418–D427, https://doi.org/10.1093/nar/gkac993 (2022).
63. Ashburner, M. *et al.* Gene Ontology: tool for the unification of biology. *Nature Genet.* **25**, 25–29, https://doi.org/10.1038/75556 (2000).
64. Kanehisa, M., Sato, Y., Kawashima, M., Furumichi, M. & Tanabe, M. KEGG as a reference resource for gene and protein annotation. *Nucleic Acids Res.* **44**, D457–D462, https://doi.org/10.1093/nar/gkv1070 (2015).
65. Li, J. *et al.* The nearly complete assembly of the *Cercis chinensis* genome and Fabaceae phylogenomic studies provide insights into new gene evolution. *Plant Commun.*, 100422, https://doi.org/10.1016/j.xplc.2022.100422 (2022).
66. Jiang, S., An, H., Xu, F. & Zhang, X. Chromosome-level genome assembly and annotation of the loquat (*Eriobotrya japonica*) genome. *GigaScience* **9**, giaa015, https://doi.org/10.1093/gigascience/giaa015 (2020).
67. Schmutz, J. *et al.* Genome sequence of the palaeopolyploid soybean. *Nature* **463**, 178–183, https://doi.org/10.1038/nature08670 (2010).
68. Liu, H. & Yi, T.-S. *unplished Lysidice rhodostegia data* (Kunming Institute of Botany, Chinese Academy of Sciences, 2024).

512 69. Young, N. D. *et al.* The *Medicago* genome provides insight into the evolution of rhizobial
513 symbioses. *Nature* **480**, 520–524, https://doi.org/10.1038/nature10625 (2011).
514 70. Kang, S.-H. *et al.* Genome-enabled discovery of anthraquinone biosynthesis in *Senna tora*.
515 *Nat. Commun.* **11**, 5875, https://doi.org/10.1038/s41467-020-19681-1 (2020).
516 71. Ai, W. *et al.* A chromosome-scale genome assembly of the Mongolian oak (*Quercus*
517 *mongolica*). *Mol. Ecol. Resour.* **22**, 2396–2410, https://doi.org/10.1111/1755-0998.13616
518 (2022).
519 72. Jaillon, O. *et al.* The grapevine genome sequence suggests ancestral hexaploidization in
520 major angiosperm phyla. *Nature* **449**, 463–467, https://doi.org/10.1038/nature06148
521 (2007).
522 73. Meng, F. *et al.* Genome assembly of *Polygala tenuifolia* provides insights into its karyotype
523 evolution and triterpenoid saponin biosynthesis. *Hortic. Res.-England* **10**, uhad139,
524 https://doi.org/10.1093/hr/uhad139 (2023).
525 74. Emms, D. M. & Kelly, S. OrthoFinder: phylogenetic orthology inference for comparative
526 genomics. *Genome Biol.* **20**, 238, https://doi.org/10.1186/s13059-019-1832-y (2019).
527 75. Shen, W., Le, S., Li, Y. & Hu, F. SeqKit: A Cross-Platform and Ultrafast Toolkit for FASTA/Q
528 File Manipulation. *PLoS One* **11**, e0163962, https://doi.org/10.1371/journal.pone.0163962
529 (2016).
530 76. Edgar, R. C. MUSCLE: multiple sequence alignment with high accuracy and high throughput.
531 *Nucleic Acids Res.* **32**, 1792–1797, https://doi.org/10.1093/nar/gkh340 (2004).
532 77. Stamatakis, A. RAxML version 8: a tool for phylogenetic analysis and post-analysis of large
533 phylogenies. *Bioinformatics* **30**, 1312–1313,
534 https://doi.org/10.1093/bioinformatics/btu033 (2014).
535 78. Minh, B. Q. *et al.* IQ-TREE 2: new models and efficient methods for phylogenetic inference
536 in the genomic era. *Mol. Biol. Evol.* **37**, 1530–1534,
537 https://doi.org/10.1093/molbev/msaa015 (2020).
538 79. Kumar, S., Stecher, G., Suleski, M. & Hedges, S. B. TimeTree: A Resource for Timelines,
539 Timetrees, and Divergence Times. *Mol. Biol. Evol.* **34**, 1812–1819,
540 https://doi.org/10.1093/molbev/msx116 (2017).
541 80. Mendes, F. K., Vanderpool, D., Fulton, B. & Hahn, M. W. CAFE 5 models variation in
542 evolutionary rates among gene families. *Bioinformatics* **36**, 5516–5518,
543 https://doi.org/10.1093/bioinformatics/btaa1022 (2020).
544 81. Chen, C. *et al.* TBtools-II: A "one for all, all for one" bioinformatics platform for biological
545 big-data mining. *Mol. Plant.* **16**, 1733–1742, https://doi.org/10.1016/j.molp.2023.09.010
546 (2023).
547 82. Sun, P. *et al.* WGDI: A user-friendly toolkit for evolutionary analyses of whole-genome
548 duplications and ancestral karyotypes. *Mol. Plant.* **15**, 1841–1851,
549 https://doi.org/10.1016/j.molp.2022.10.018 (2022).
550 83. Camacho, C. *et al.* BLAST+: architecture and applications. *BMC Bioinformatics* **10**, 421,
551 https://doi.org/10.1186/1471-2105-10-421 (2009).

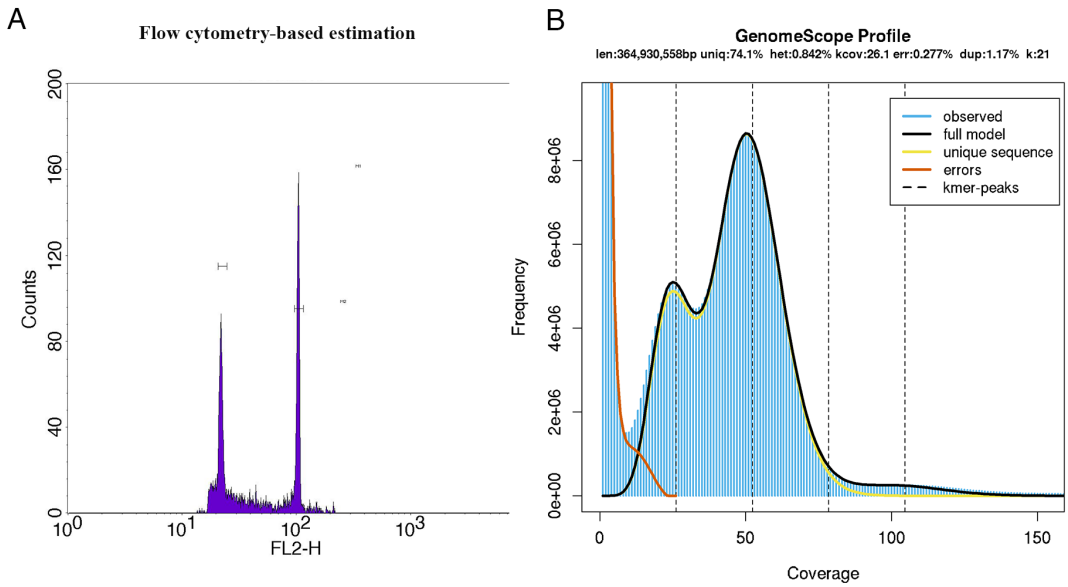

Figure 1 The result of genome size estimation for *Z. insignis*. (A) Flow cytometry-based estimation result of *Z. insignis* (left peak, the sample) and *Zea mays* (right peak, the reference). (B) The 21-*kmer* distribution estimation result was obtained using GenomeScope2. The distribution of *21-kmer* exhibited two major peaks, indicating certain heterozygosity within the genome, and high-frequency *k-mers* with coverage near 1 that was possibly generated by sequencing errors.

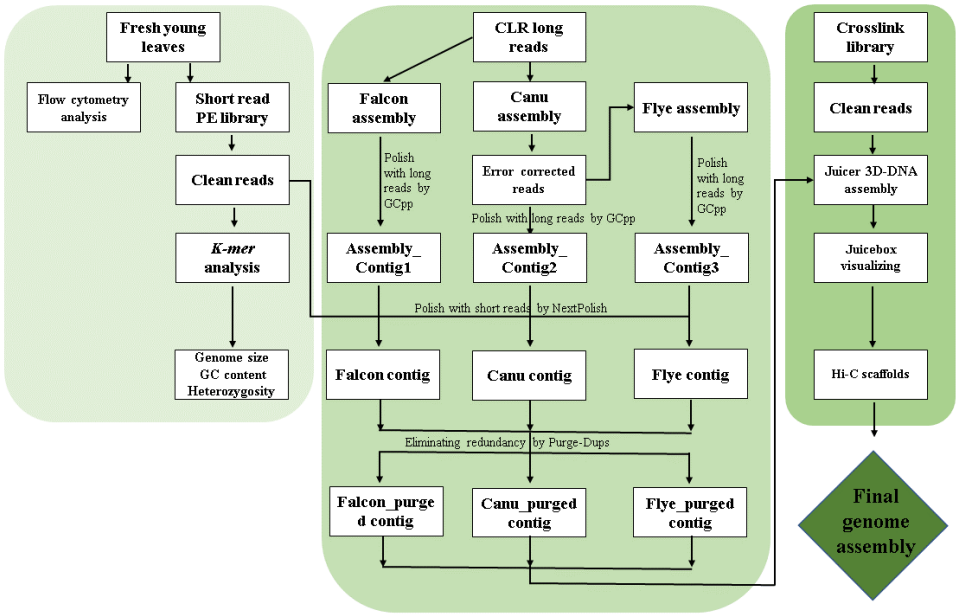

Figure 2 The pipeline for the chromosome-level genome assembly of *Z. insignis*.

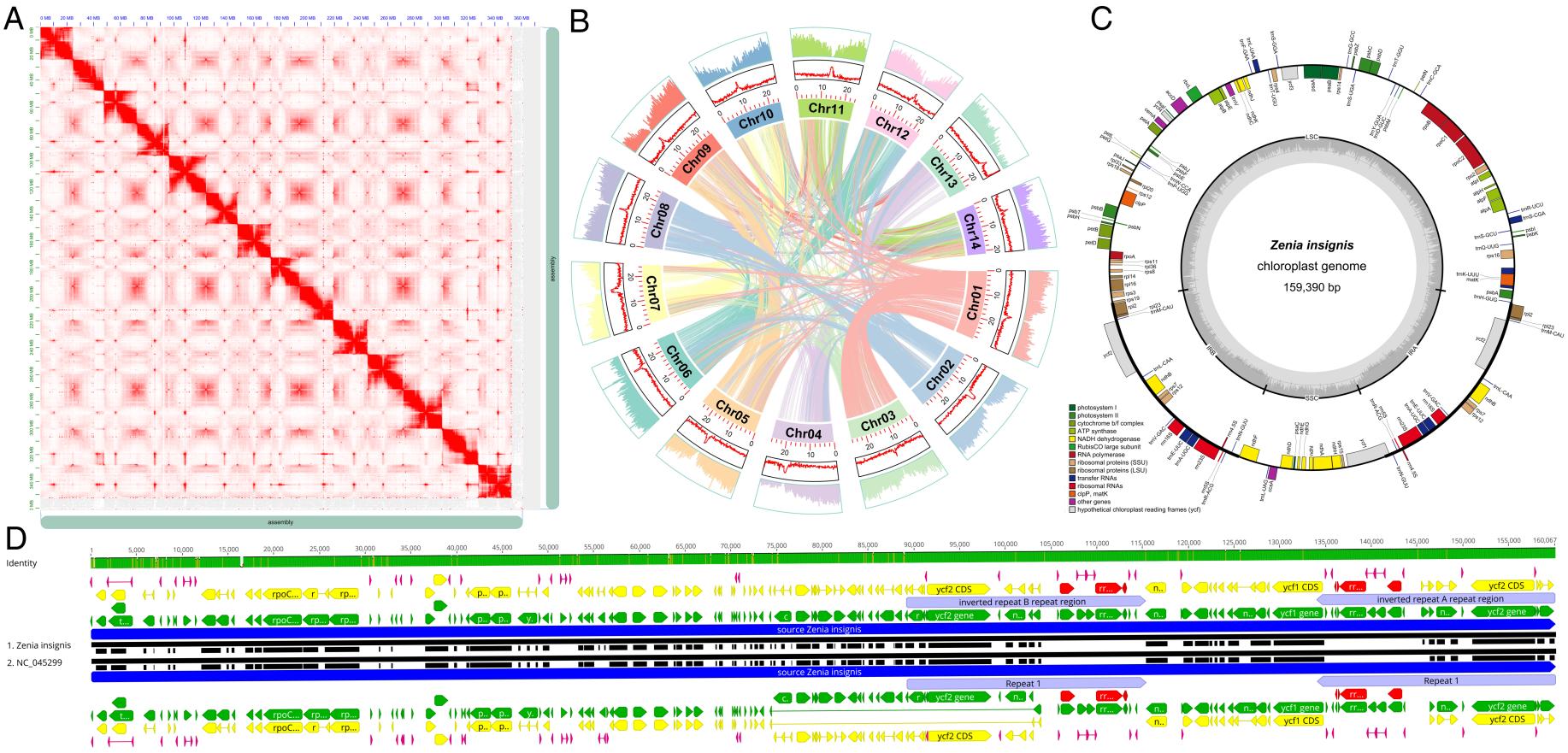

Figure 3 The chromosome and plastome information of *Z. insignis*. (A) The interaction heat map of Hi-C among chromosomes for the *Z. insignis* genome. The Hi-C interaction matrix shows the pairwise correlations among the 14 pseudomolecules. (B) The high-quality genomic landscape of *Z. insignis*. The genome diagram has four circles from the outside: gene density, GC content, chromosomal length, and intraspecies collinearity. (C)The

565 visualization of the plastome genome of *Z. insignis* using OGDRAW. The outside circle displays genes color-coded according to their functional
566 groups. The second circle illustrates the large single-copy (LSC), inverted repeat (IRA, IRB), and small single-copy (SSC) regions. The third circle
567 delineates the percentage of GC content and genomic positions in kilobase pairs. (D) Compared analysis of plastome for *Z. insignis*. Gene(green),
568 CDS (yellow), RNA (red), and IR regions (grey) have been color-coded according to their functional groups. The identity of the two plastome
569 sequences exhibited high overall similarity, except for some regions in non-coding sequences.

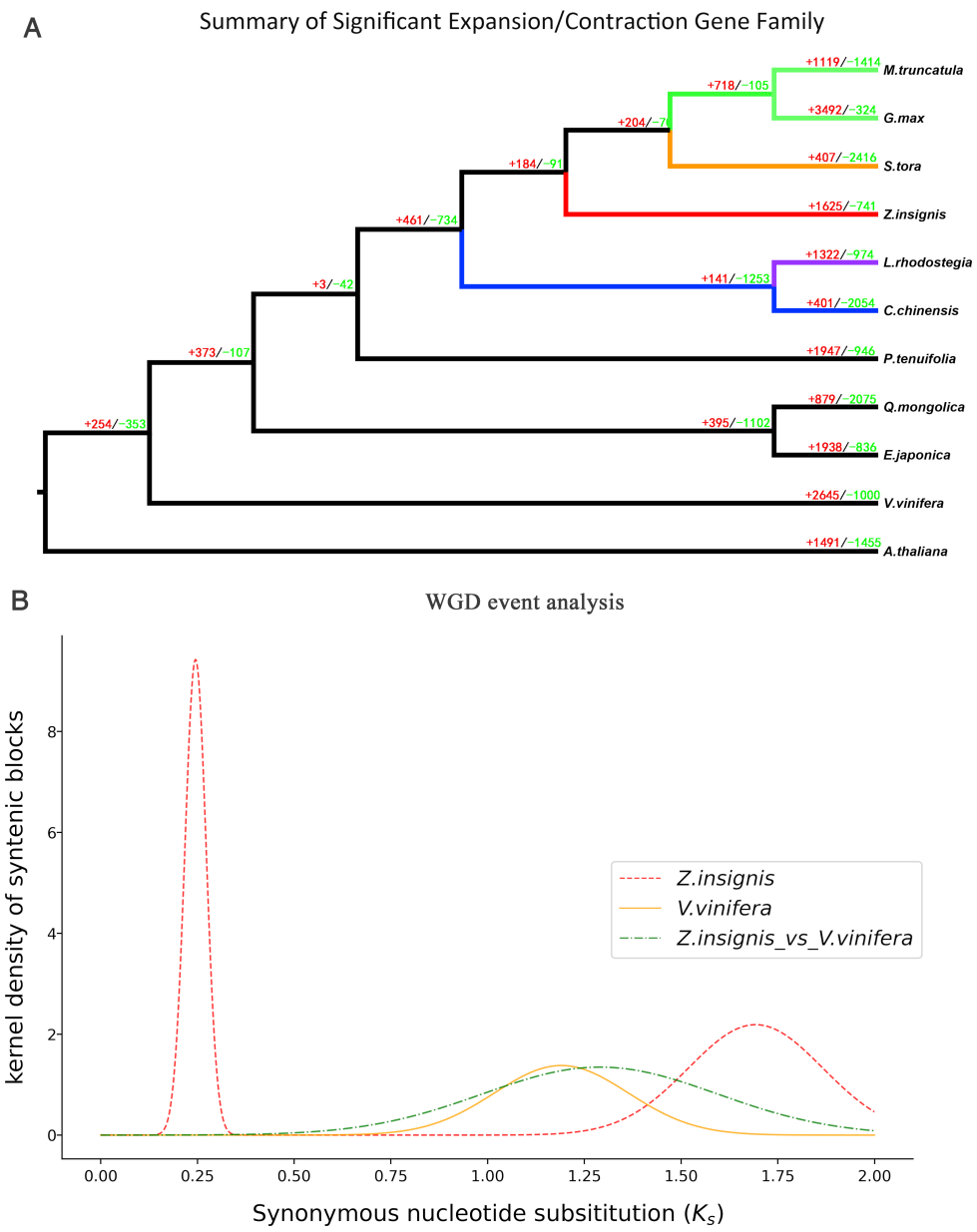

Figure 4 The result of Gene family evolution and distribution of *Ks* values. (A) The result of gene family evolution. The plus/minus sign corresponding numbers reflect the expansion or contraction of gene families. The color of the branch indicates different subfamilies of Fabaceae. (B) The distribution of *Ks* values between *Z. insignis* and *V. Vinifera*. The *Ks* distribution curve of *Z. insignis, V. Vinifera, and Z. insignis vs. V. Vinifera* exhibited a significant overlap in the right *Ks* peak.

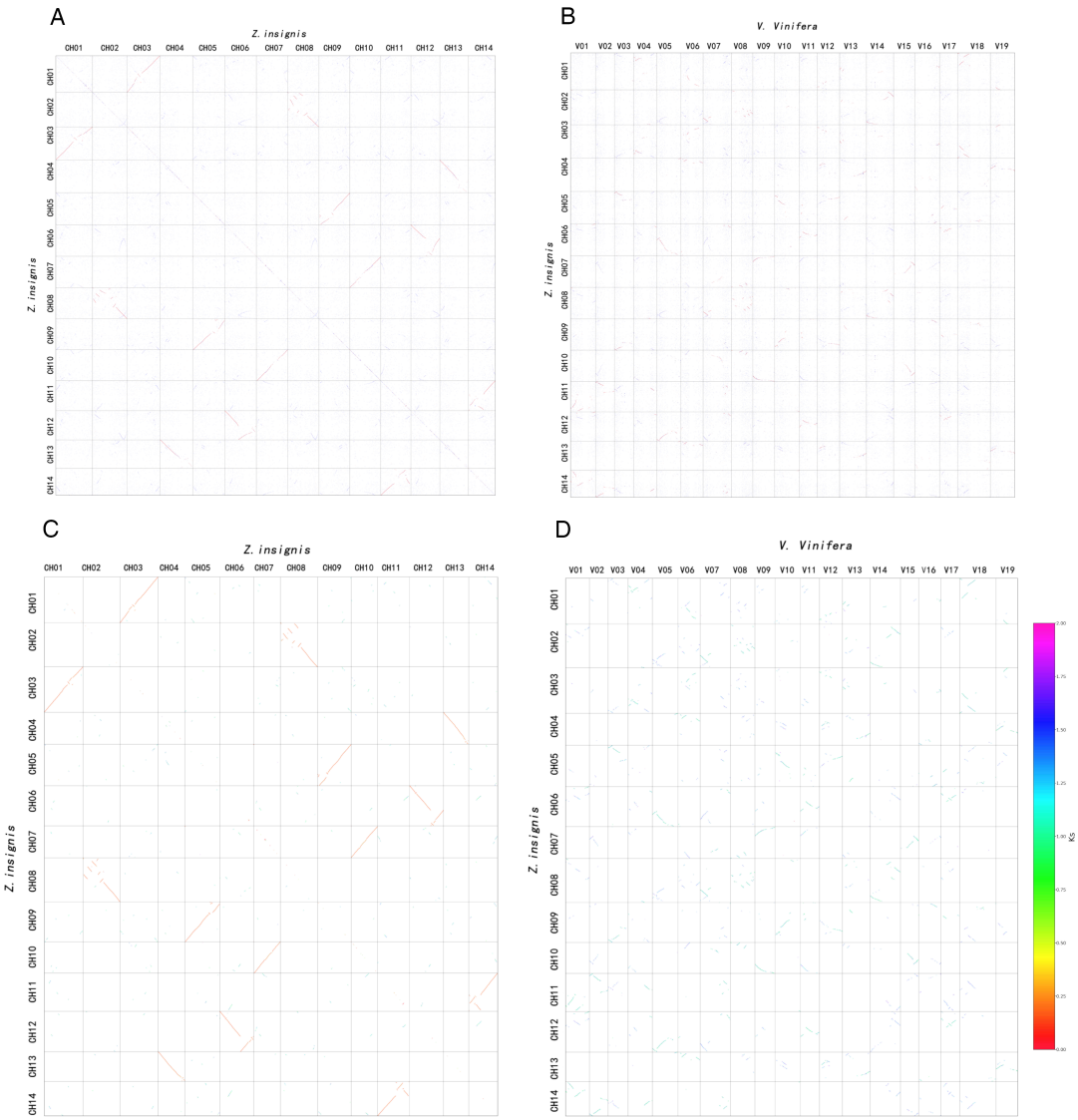

Figure 5. The result of WGDI analysis for *Z. insignis*. (A) The homologous genes dot plot of genomic synteny between chromosomes of *Z. insignis*. The best-hit genes are indicated in red, the second best-hit genes are in blue, and the other hit genes are in gray. (B) Dot plot of genomic synteny between *Z. insignis* and *V. Vinifera*. The best-hit genes are indicated in red, the second best-hit genes in blue, and the other hit genes are in gray (C) *Ks* dot plot of genomic synteny between chromosomes of *Z. insignis*. The color of the dot indicates the *Ks* of the gene pair. (B) *Ks* dot plot of genomic synteny between *Z. insignis* and *V. Vinifera*. The color of the dot indicates the *Ks* of the gene pair.

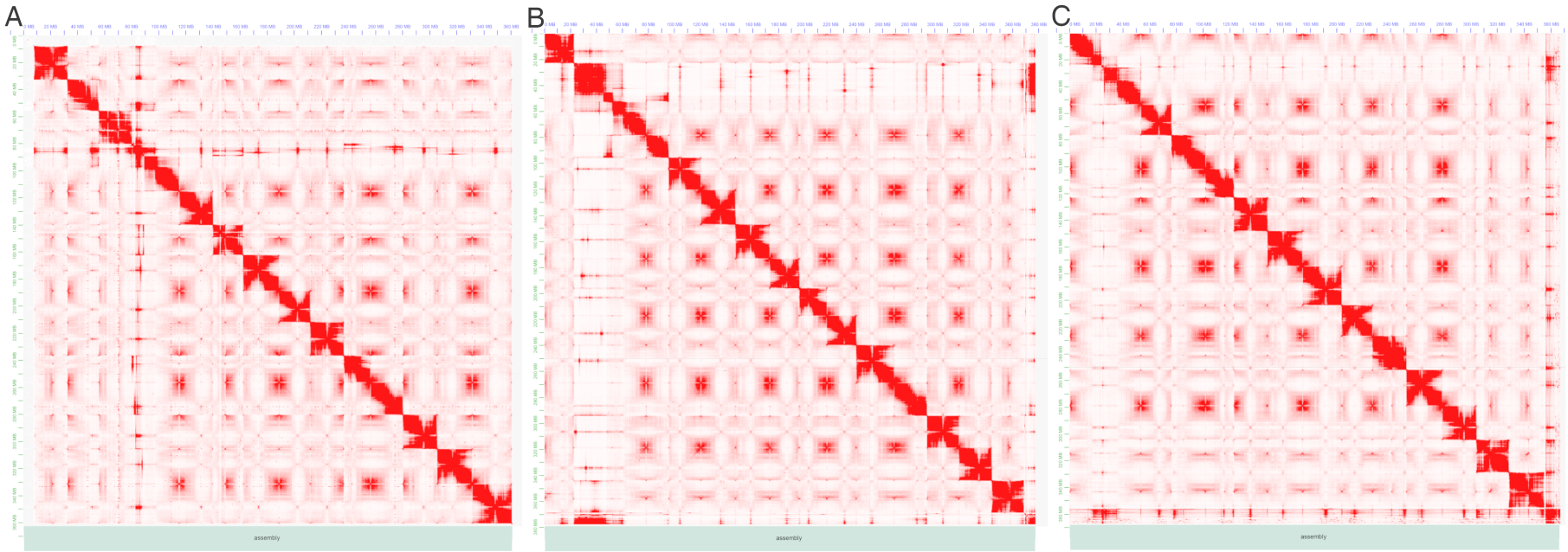

Supplementary Figure 1 The heat map of the Hi-C interaction matrix generated by Purge_Dups. (A) Heat map of Hi-C for Falcon_purge. (B) Heat map of Hi-C for Canu_purge. (C) The Heat map of Hi-C for Flye_purge.

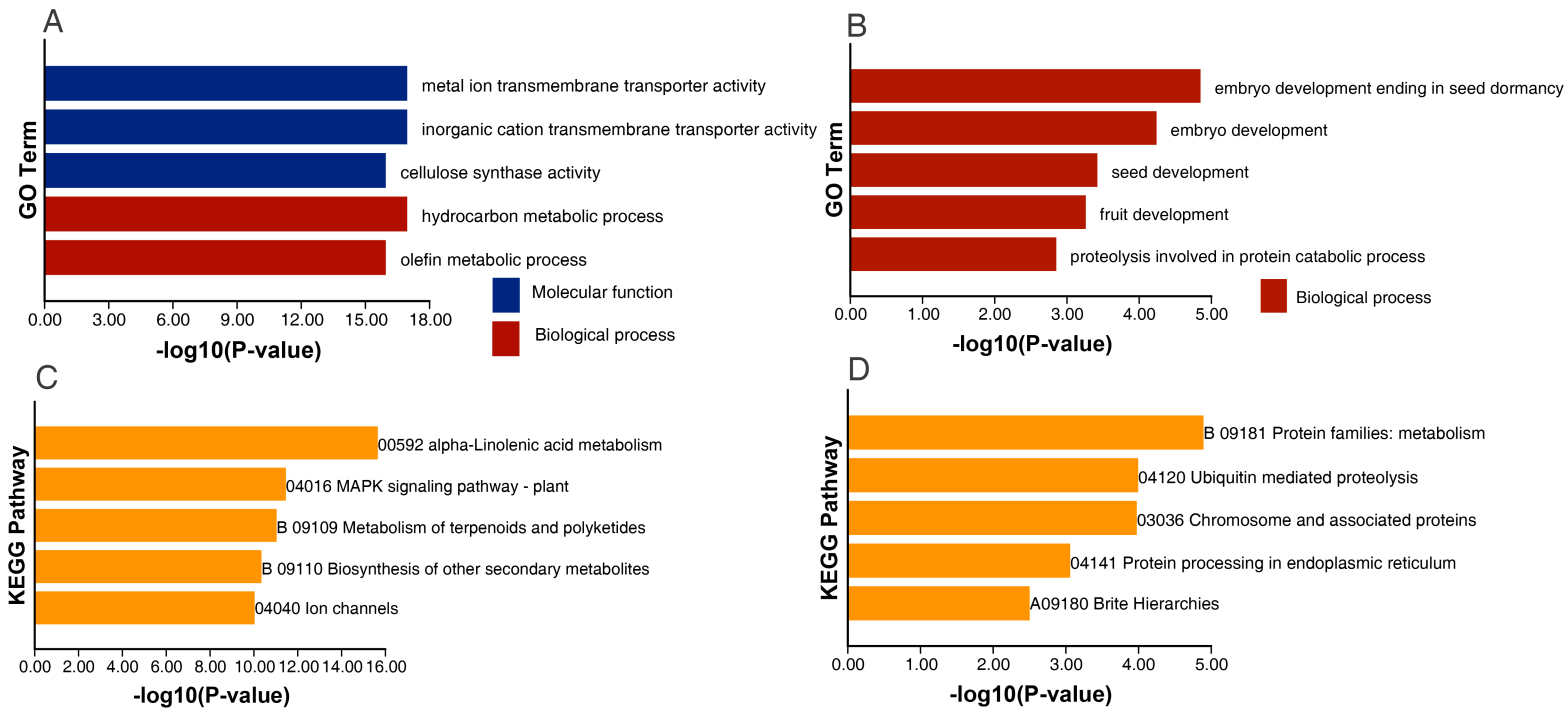

Supplementary Figure 2 The result of enrichment analyses for GO and KEGG. (A)The result of GO enrichment analyses for significant expansion gene families. (B) The result of GO enrichment analyses for significant contraction gene families. (C) The result of KEGG enrichment analyses for significant expansion gene families. (B) The result of KEGG enrichment analyses for significant contraction gene families.

Table 1 Statistics of sequencing data

Survey data	PacBio CCS data	Hi-C data	Full-length Transcriptome data
44140.85Mb	174,139.06Mb	59,630.13Mb	81.92Mb
91.96×	363.43×	124.45×	—

Table 2 The results of the assessment for N50

	Canu_contig		Canu_purged_contig		Falcon_contig		Falcon_purged_contig		Flye_contig		Flye_purged_contig	
Nx	Size	Number	Size	Number	Size	Number	Size	Number	Size	Number	Size	Number
N90	92660	1400	1431948	43	363551	152	1503027	68	172335	253	309802	192
N80	113319	822	4428622	31	1150475	87	2685811	49	529601	137	653152	114
N70	156297	367	7093928	23	2280795	59	3819453	38	952759	84	1139158	72
N60	320232	71	8669316	18	3626040	43	4916748	29	1478745	53	1600360	46
N50	4693084	29	10026892	14	4819753	31	6024120	22	2345742	32	2516555	29
N40	7292602	20	12366826	11	5750257	23	7011975	17	3977660	20	4128350	18
N30	10196961	13	14068457	8	7098875	16	7310681	12	6920119	12	7140693	11
N20	14068457	8	14855825	5	7527208	9	8509734	7	9355035	7	9355035	7
N10	15123523	4	15261855	3	9877742	4	11240351	3	9936040	4	10281987	3
TotalLength	592944931	2337	377600313	448	457757591	598	360998718	266	371463918	1303	354656638	744

Table 3 The results of the assessment for BUSCO

	Canu_contig	Canu_purged_contig	Falcon_contig	Falcon_purged_contig	Flye_contig	Flye_purged_contig
Complete BUSCOs (C)	98.50%	98.50%	97.50%	97.30%	98.60%	98.60%
Complete and single-copy BUSCOs (S)	44.10%	77.30%	65.80%	79.80%	76.70%	76.90%
Complete and duplicated BUSCOs (D)	54.40%	21.20%	31.70%	18.40%	21.90%	21.70%
Fragmented BUSCOs (F)	0.30%	0.60%	1.00%	1.20%	0.40%	0.60%
Missing BUSCOs (M)	1.20%	0.90%	1.50%	1.50%	1.00%	0.80%
Total BUSCO groups	1614	1614	1614	1614	1614	1614

599 Table 4 The results of the assessment for LAI

	Chromosome From	To	Intact	Total	raw_LAI	LAI
Canu_contig	1	592944931	0.0088	0.2003	4.38	0
Canu_purged_contig	1	377600313	0.0126	0.2099	5.98	11.61
Falcon_contig	1	457757591	0.0077	0.1684	4.57	4.62
Falcon_purged_contig	1	360998718	0.0119	0.1329	8.94	14.57
Flye_contig	1	371463918	0.0109	0.1868	5.83	11.46
Flye_purged_contig	1	354656638	0.0108	0.1689	6.4	12.03

600 Table 5 The result of repeat sequences annotation

Type	Length(bp)	Rate (%)
DNAs	11129683	3.08
LINEs	6520335	1.81
SINEs	298378	0.08
LTRs	32617056	9.03
Rolling-circles	1280052	0.35
Small RNA	6975086	1.93
Satellites	0.00	0.00
Simple repeats	3559151	0.99
Low complexity	1063047	0.29
Unknown	64922128	17.98
Total	128083818	35.47

601 Table 6 The result of BUSCO for gene prediction

	R1	R2	R3	R3+PASA
Complete BUSCOs (C)	46.60%	96.60%	96.80%	97.20%
Complete and single-copy BUSCOs (S)	39.90%	44.80%	43.90%	44.20%
Complete and duplicated BUSCOs (D)	6.70%	51.80%	52.90%	53.00%
Fragmented BUSCOs (F)	3.50%	2.30%	2.30%	1.90%
Missing BUSCOs (M)	49.90%	1.10%	0.90%	0.90%
Total BUSCO groups	1614	1614	1614	1614

602